

# Arteriosclerosis, Thrombosis, and Vascular Biology

JOURNAL OF THE AMERICAN HEART ASSOCIATION

American Heart  
Association®



*Learn and Live* SM

## **Ninein Is Expressed in the Cytoplasm of Angiogenic Tip-Cells and Regulates Tubular Morphogenesis of Endothelial Cells**

Taro Matsumoto, Petter Schiller, Lothar C. Dieterich, Fuad Bahram, Yuji Iribe, Ulf Hellman, Charlotte Wikner, Gordon Chan, Lena Claesson-Welsh and Anna Dimberg  
*Arterioscler. Thromb. Vasc. Biol.* 2008;28;2123-2130; originally published online Sep 4, 2008;

DOI: 10.1161/ATVBAHA.108.169128

Arteriosclerosis, Thrombosis, and Vascular Biology is published by the American Heart Association,  
7272 Greenville Avenue, Dallas, TX 75214

Copyright © 2008 American Heart Association. All rights reserved. Print ISSN: 1079-5642. Online  
ISSN: 1524-4636

The online version of this article, along with updated information and services, is  
located on the World Wide Web at:

<http://atvb.ahajournals.org/cgi/content/full/28/12/2123>

Subscriptions: Information about subscribing to Arteriosclerosis, Thrombosis, and Vascular  
Biology is online at

<http://atvb.ahajournals.org/subscriptions/>

Permissions: Permissions & Rights Desk, Lippincott Williams & Wilkins, a division of Wolters  
Kluwer Health, 351 West Camden Street, Baltimore, MD 21202-2436. Phone: 410-528-4050. Fax:  
410-528-8550. E-mail:

[journalpermissions@lww.com](mailto:journalpermissions@lww.com)

Reprints: Information about reprints can be found online at

<http://www.lww.com/reprints>

# Ninein Is Expressed in the Cytoplasm of Angiogenic Tip-Cells and Regulates Tubular Morphogenesis of Endothelial Cells

Taro Matsumoto, Petter Schiller, Lothar C. Dieterich, Fuad Bahram, Yuji Iribe, Ulf Hellman, Charlotte Wikner, Gordon Chan, Lena Claesson-Welsh, Anna Dimberg

**Objective**—Angiogenesis is an integral part of many physiological processes but may also aggravate pathological conditions such as cancer. Development of effective angiogenesis inhibitors requires a thorough understanding of the molecular mechanisms regulating vessel formation. The aim of this project was to identify proteins that regulate tubular morphogenesis of endothelial cells.

**Methods and Results**—Phosphotyrosine-dependent affinity-purification and mass spectrometry showed tyrosine phosphorylation of ninein during tubular morphogenesis of endothelial cells. Ninein was recently identified as a centrosomal microtubule-anchoring protein. Our results show that ninein is localized in the cytoplasm in endothelial cells, and that it is highly expressed in the vasculature in normal and pathological human tissues. Using embryoid bodies as a model of vascular development, we found that ninein is abundantly expressed in the cytoplasm of endothelial cells during sprouting angiogenesis, in particular in the sprouting tip-cell. In accordance, siRNA-dependent silencing of ninein in endothelial cells inhibited tubular morphogenesis.

**Conclusions**—In this study, we show that ninein is expressed in developing vessels and in endothelial tip cells, and that ninein is critical for formation of the vascular tube. These data strongly implicate ninein as an important new regulator of angiogenesis. (*Arterioscler Thromb Vasc Biol.* 2008;28:2123-2130.)

**Key Words:** ninein ■ angiogenesis ■ tubular morphogenesis ■ microtubule ■ endothelial

There is a well-established relationship between excess angiogenesis and progression of cancer and other pathological conditions, as well as impaired vascularization in ischemic conditions. This implies that anti- or proangiogenic treatments may be beneficial as a complement to existing therapies for a wide range of diseases. Development of efficient drugs that target the vasculature requires delineation of mechanisms that regulate blood vessel formation. The critical importance of growth factors and signal transduction by their cognate receptors, including vascular endothelial growth factors (VEGFs) and fibroblast growth factors (FGFs) in regulation of angiogenesis is widely recognized.<sup>1,2</sup> However, we still need to identify their downstream molecular targets that regulate different aspects of the fine-tuned response resulting in formation of new vessels.

## See accompanying article on page 2094

In the adult, new blood vessels form through distinct and overlapping mechanisms, depending on the microenvironment and the molecular context.<sup>3-5</sup> Sprouting angiogenesis is

initiated when endothelial cells are stimulated by angiogenic growth factors eg, VEGF. The endothelial cells degrade the basement membrane of preexisting vessels, migrate into the surrounding matrix, proliferate, and finally differentiate to new, lumen containing vessels. Circulating endothelial cells or progenitors may contribute to a variable extent, forming new vessels through a process that largely resembles embryonic vasculogenesis. Finally, the newly formed vessel deposits a vascular basement membrane, and recruits stabilizing pericytes.

To define the proteome regulating endothelial differentiation to lumen-containing vessels, we used an in vitro model of tubular morphogenesis and screened for proteins that were tyrosine phosphorylated during this process. One of the identified phosphoproteins was ninein, a protein that has been shown to be involved in the minus-end anchoring of microtubules in the centrosome.<sup>6-8</sup> In this study, we have analyzed expression of ninein in several types of endothelial cells in vitro and in vivo, and used advanced cell culture models to evaluate the role of ninein in blood vessel formation.

Original received April 23, 2008; final version accepted August 26, 2008.

From the Department of Genetics and Pathology (T.M., P.S., L.C.D., F.B., C.W., L.C.-W., A.D.), Uppsala University, Rudbeck Laboratory, Sweden; the Division of Cell Regeneration and Transplantation, Advanced Medical Research Center (T.M., Y.I.), Nihon University School of Medicine, Tokyo, Japan; the Ludwig Institute for Cancer Research, Uppsala Branch, Biomedical Center (U.H.), Uppsala, Sweden; and the Department of Oncology (G.C.), University of Alberta, Experimental Oncology, Cross Cancer Institute, Edmonton, Alberta, Canada.

Correspondence to Anna Dimberg, Department of Genetics and Pathology, Rudbeck Laboratory, S-751 85 Uppsala, Sweden. E-mail Anna.Dimberg@genpat.uu.se

© 2008 American Heart Association, Inc.

*Arterioscler Thromb Vasc Biol* is available at <http://atvb.ahajournals.org>

DOI: 10.1161/ATVBAHA.108.169128

## Methods

### Cell Culture and In Vitro Angiogenesis Assays

Bovine capillary endothelial (BCE) cells from calf adrenal cortex were maintained in DMEM (Life Technologies), 10% newborn calf serum (NCS), and 2 ng/mL fibroblast growth factor-2 (FGF-2, Boehringer). Tubular morphogenesis was induced in a three-dimensional (3D) collagen matrix in DMEM containing 10% NCS and 10 ng/mL FGF-2, as described.<sup>9</sup> Telomerase-immortalized human microvascular endothelial (TIME) cells<sup>10</sup> were cultured in EBM MV2 medium with supplements (5 ng/mL EGF, 0.2 μg/mL hydrocortisone, 0.5 ng/mL VEGF-A, 10 ng/mL FGF-2, 20 ng/mL IGF-1; Promocell). Tube formation was induced in 3D collagen gels by 50 ng/mL VEGF-A (PeproTech) in EBM MV2 medium, 2% fetal bovine serum (FBS) as described.<sup>11</sup> Mouse ES cell line R1<sup>12</sup> was maintained on growth-arrested mouse embryonic fibroblasts in DMEM-Glutamax medium supplemented with 15% FBS, 25 mmol/L HEPES pH 7.4, 1.2 mmol/L sodium pyruvate, 0.12% monothiolglycerol and 1000 U/mL leukemia inhibitory factor. Embryoid bodies were induced as described<sup>13</sup> in the presence of VEGF-A (30 ng/mL, PeproTech), seeded in 8-well tissue-culture slides or in a 3D-collagen matrix to induce formation of endothelial sprouts and analyzed at day 8 or 12.<sup>13</sup> Porcine aortic endothelial (PAE) cells and human 293T cells were maintained in DMEM with 10%FBS, and human U2OS cells were maintained in RPMI with 10%FBS.

### Cell Lysates and Western Blot Analysis

Cells were washed in PBS and lysed in boiling SDS sample buffer or in a modified RIPA buffer (1% Triton X-100, 40 mmol/L Tris-HCl, pH 8, 0.1% SDS) with complete protease inhibitor (Roche Applied Science). Extracts were fractionated on Novex NuPAGE (3% to 8% Tris-acetate) precast gels (Invitrogen). The membrane (Hybond-C extra, GE Healthcare) was blocked in 5% dry milk in 0.1% Tween, Tris-buffered saline (TTBS), and Western blot analysis was done as described.<sup>9</sup> Primary antibodies used were: antiphosphotyrosine antibody 4G10 (Upstate Biotechnology), anti-β-catenin (Transduction Laboratories), antininein produced in-house,<sup>14</sup> and antininein (Biologend).

### Purification and Identification of Phosphotyrosyl Proteins in Differentiating BCE Cells

Briefly, serum-starved BCE cells were cultured on collagen gels or gelatinized dishes and incubated in DMEM containing 10% NCS and 10 ng/mL FGF-2 for 24 hours at 37°C. Cells were lysed and phosphotyrosine-containing proteins were immunoprecipitated using an antiphosphotyrosine (4G10)-agarose conjugate (Upstate Biotechnology). Proteins were separated by SDS-PAGE, the gel was silver stained, and protein bands were extracted by in-gel digestion. Identification of proteins was done using a Bruker Biflex III MALDI-TOF-MS (Bruker Daltonics). For a full description of methods involved, please see <http://atvb.ahajournals.org>.

### Immunofluorescence

BCE cells, TIME cells, or embryoid bodies were washed in TBS, fixed for 30 minutes at rt or at 4°C overnight in zinc fix (0.1 mol/L Tris-HCl, pH 7.5, 3 mmol/L calcium acetate, 23 mmol/L zinc acetate, 37 mmol/L zinc chloride) containing 0.2% Triton X-100, blocked in 3% BSA in TBS for 1 hour at rt, and incubated with primary antibodies in blocking solution for 2 hours at rt. Samples were washed in TBS and incubated with Alexa-conjugated secondary antibodies (Molecular Probes) and/or phalloidin-Texas Red (Molecular Probes) in blocking solution for 1 hour at rt, followed by Hoechst 33342 nuclear staining.

Fully anonymized tissue samples were used in accordance with the Swedish biobank legislation. The use of human tissue was approved by the Ethical Review Board in Uppsala (No. Ups 03-412/2003). Frozen sections (6 μm) were obtained from the Fresh Tissue Biobank, Uppsala University Hospital; renal carcinoma (n=5) and normal kidney (n=4). Methanol-fixed sections were blocked in 3%

BSA and then incubated with primary antibodies in blocking solution for 2 hours at rt. The sections were washed in PBS and incubated with Alexa-conjugated secondary antibodies (Molecular Probes) or Fluorescein Ulex Europeus Agglutinin-I (fluorescein isothiocyanate [FITC]-UEA-1, Vector Laboratories), followed by nuclear staining with Hoechst 33342. Primary antibodies used were: antininein,<sup>14</sup> anti-β-tubulin (Molecular Probes), anti-γ-tubulin (Sigma), anti-CD31 (BD Biosciences) and antinerve glia 2 (NG2) (Chemicon).

### Ninein-GFP cDNA Transfection

PAE and 293T cells were transfected with vectors encoding green fluorescent protein (GFP; pMaxGFP, Amaxa, Cologne, Germany) or ninein fused to GFP (ninein-GFP,<sup>15</sup> a kind gift from Dr Michel Bornens, Institute Curie, Paris, France) using Lipofectamine (Invitrogen) according to the manufacturer's instructions.

### In Situ Proximity Ligation

TIME cells were plated on gelatinized 8-well culture slides and cultured in EBM MV2 medium with supplements for 48 hours and fixed in 2% paraformaldehyde, 15 minutes on ice. Tyrosine phosphorylated ninein was detected by the Proximity Ligation Assay (OLINK), through oligonucleotide-conjugated secondary antibodies. Close proximity of the secondary antibodies allows a rolling-circle amplification, detected by use of Texas Red-labeled probe (see [www.olink.com](http://www.olink.com)). Primary antibodies used were rabbit-antininein (Abcam), combined with either mouse monoclonal antiphosphotyrosine 4G10 (Upstate Biotechnology) or mouse monoclonal antiphosphotyrosine p-Tyr-100 (Cell Signaling). As a negative control, a rabbit-anti-HA (human influenza hemagglutinin) antibody (Santa Cruz Biotechnology) was used in combination with a mouse antininein antibody.<sup>14</sup>

### Ninein siRNA Transfection

TIME cells were seeded in 6-well tissue culture dishes 24 hours before transfection with siRNA targeting ninein (Nin-1, Nin-2) or control siRNA (Medium GC-content Stealth RNAi Negative control, Invitrogen) using Lipofectamine RNAiMAX Reagent (Invitrogen). At 48 hours posttransfection, cells were seeded on collagen matrices in 12-well plates for tube formation as described above. After 24 hours, tubular structures were fixed using zinc-fix containing 0.2% Triton X-100 and incubated with Texas Red-phalloidin (Molecular Probes) and Hoechst 33342. Samples were examined using a Nikon Eclipse E1000 microscope (Nikon). Images from 10× or 4× optical fields spanning the tube-forming area of each well were analyzed using Easy Image Analysis 2000 software (Rainfall). Total area of tubular structures were calculated, and the values of Nin-1 and Nin-2 treated cells were compared to nonsilencing control siRNA-treated cells.

Ninein targeting Stealth RNAi Duplexes (Invitrogen) used were:

Nin-1: Sense: ACAAGAAGACAUUACUAACCCUGGC

Antisense: GCCAGGGUAGUAAUGUCUUCUUGU

Nin-2: Sense: UUUAACUUCAGAGAGCUCGCCUCC

Antisense: GGAGGCGGAGCUCUCUGAAGUUAAA

Immunohistochemical and immunofluorescence microscopy

Samples were mounted using Fluoromount-G (Southern Biotech) and analyzed using a Nikon Eclipse E100 microscope (Nikon; Figure 4A), a Nikon TE300 Eclipse inverted fluorescence microscope (Nikon; Figure 1A, 6D upper panel), or an LSM 510 META confocal laser-scanning inverted microscope (Carl Zeiss International, Oberkochen, Germany; Figures 2A through 2E, 3, 4A through 4D, 5B through 4E, and 6D, lower panel). The following objectives were used: Nikon Plan Apochromat 4×/0.2, 10×/0.45, 20×/0.75; Nikon TE300 Eclipse Plan Fluor 10×/0.3; Zeiss confocal Plan Neofluar 20×/0.75 UV Plan Apochromat 63×/1.4 oil immersion 100×/1.45 oil immersion. Microphotographs were captured using a Nikon Eclipse DXM 1200 camera or a Spot camera (Diagnostic Instruments, Inc).

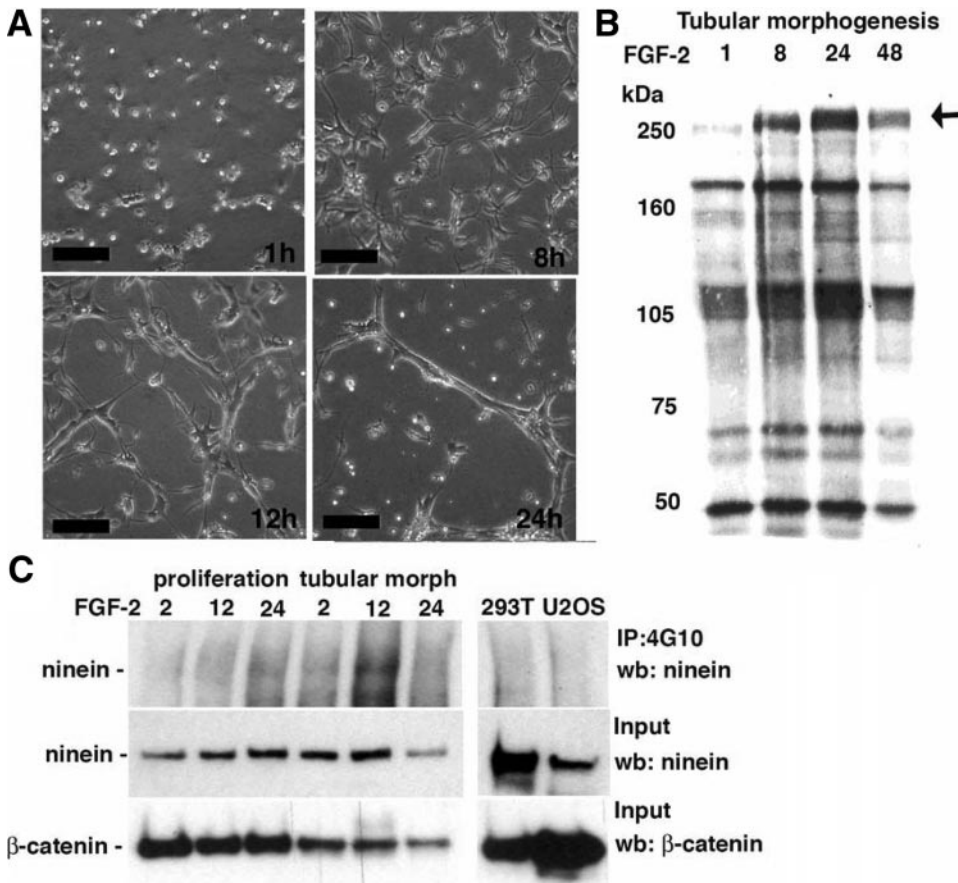


**Figure 1.** Ninein tyrosine phosphorylation during tubular morphogenesis. A, Tubular morphogenesis of BCE cells by FGF-2 in 3D-collagen. Bar=50  $\mu$ m. B, BCE cells forming tubular structures at 1, 8, 24, and 48 hours analyzed by immunoblotting using antiphosphotyrosine 4G10. C, Immunoprecipitation of phosphotyrosine-proteins followed by immunoblotting for ninein.

**Statistical Examination**

Statistical examination was performed on all data using ANOVA or unpaired Student *t* test using the Statview software. We considered a probability value less than 0.05 to be significant.

**Results**

To identify proteins that participate in formation of the vascular tube during angiogenesis, we used primary bovine capillary endothelial cells (BCE) that form vessel-like structures when cultured in a 3D-collagen matrix in the presence of FGF-2 (Figure 1A). Tyrosine phosphorylation is a hallmark of growth factor action. Western blot analysis of whole-cell lysates collected at different times visualized several proteins that were tyrosine phosphorylated during tubular morphogenesis (Figure 1B). In particular, we found a striking regulation of a prominent component of about 250 kDa (arrow). To allow further molecular characterization, tyrosine phosphorylated proteins retrieved from FGF-2-treated endothelial cells undergoing tubular morphogenesis were affinity purified using an antiphosphotyrosine-antibody column. Eluted proteins were separated by SDS-acrylamide gel electrophoresis. Silverstaining of the gel showed components with a relative migration rate of about 250 kDa, specifically induced in the FGF-2-treated condition. This region of the gel was cut out, subjected to in-gel trypsin-digestion and mass spectrometry. Using this strategy, we identified 3 proteins whose molecular mass is compatible with a relative migration rate of about 250 kDa: filamin, nonmuscle myosin, and ninein.

We compared expression and activation of these proteins in extracts from BCE cells forming tubular structures in a 3D-collagen matrix or proliferating on gelatin. Immunoprecipitation with antiphosphotyrosine antibodies confirmed that ninein and nonmuscle myosin were tyrosine phosphorylated during tubular morphogenesis, with a maximal level of phosphorylation at 12 hours (Figure 1C and data not shown). There was a slight phosphorylation of ninein also in the proliferating cells. The level of ninein expression increased during tubular morphogenesis as compared to proliferating cells (compare with  $\beta$ -catenin loading control; Figure 1C). Tyrosine phosphorylation of ninein was also detected when examining telomerase-immortalized human microvascular endothelial (TIME) cells forming tubular structures in a 3D-collagen matrix in response to VEGF (data not shown). Importantly, ninein was not tyrosine phosphorylated in human fibroblast 293T cells or in human osteosarcoma U2OS cells (Figure 1C). We could not confirm tyrosine phosphorylation of filamin (data not shown), suggesting that filamin may be indirectly retained on the affinity-column through interaction with another phosphorylated protein.

The potential role of ninein during angiogenesis has not previously been investigated. Ninein was initially identified as a centrosome-marker, important for minus-end anchoring of microtubuli.<sup>6,8,16</sup> Whereas immunofluorescence analysis showed ninein colocalized with the centrosomal marker  $\gamma$ -tubulin in nonendothelial cells, including U2OS and 293T, ninein was found both in the centrosome and throughout the

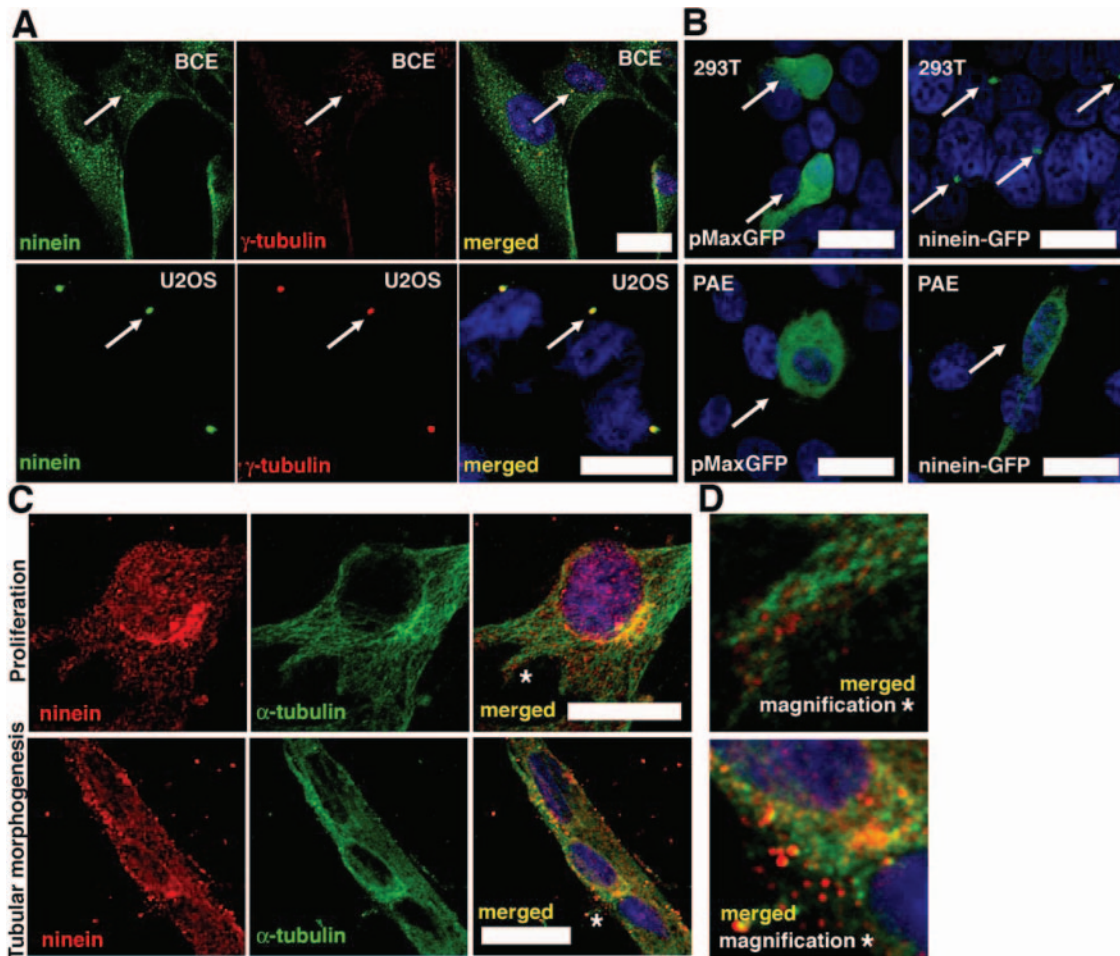


**Figure 2.** Ninein localization. A, Localization of ninein (green) and  $\gamma$ -tubulin (red) in BCE and U2OS cells. B, Expression of ninein-GFP (right) or GFP (pMaxGFP, left) in 293T and PAE cells. C, Immunostaining of ninein (red) and  $\alpha$ -tubulin (green) in BCE cells proliferating on gelatin (upper) or forming tubular structures in 3D-collagen (lower). \*Area magnified in D. Bars=20  $\mu$ m.

cytoplasm in endothelial cells of different species, including BCE (Figure 2A), PAE (supplemental Figure IA, available online at <http://atvb.ahajournals.org>), and TIME cells (data not shown). The cytoplasmic localization of ninein in endothelial cells was confirmed by transfecting PAE cells with a vector encoding ninein tagged with GFP, which resulted in cytoplasmic localization of the ninein-GFP fusion protein. In contrast, transfection of 293T cells with the ninein-GFP vector resulted in expression exclusively in centrosomes (Figure 2B, right panels). As expected, transfection of a vector expressing GFP alone resulted in cytoplasmic localization of GFP in both cell types (pMaxGFP; Figure 2B, left panels). The cytoplasmic distribution of ninein differed depending on the endothelial cell program. Thus, during FGF-2-induced proliferation of BCE cells cultured on gelatin, ninein was partially colocalized with the microtubular cytoskeleton (Figure 2C and 2D, top panels). This is in accordance with a previous report that demonstrated ninein traveling along microtubules to noncentrosomal sites during epithelial differentiation.<sup>17</sup> However, when BCE cells formed tubular structures in a collagen matrix, microtubular structures were less elaborate and both ninein and tubulin were found distributed throughout the cytoplasm (Figure 2C and

2D, bottom panels). Cytoplasmic localization of ninein was consistently found throughout the tubular structures (supplemental Figure IB, please see <http://atvb.ahajournals.org>).

To determine the subcellular localization of tyrosine phosphorylated ninein in endothelial cells, we used the proximity ligation methodology, using oligonucleotide-conjugated secondary antibodies which when in close proximity allow an in situ PCR reaction. This is a sensitive method eg, for detection of protein modifications such as phosphorylation. Combining ninein primary antibodies with either of two different phospho-tyrosine antibodies (4G10 or p-Tyr-100) resulted in the detection of Texas Red-labeled RCA products (indicative of phosphorylated ninein) in the cytoplasm of TIME cells (supplemental Figure IIA). VEGF-A induced an additional 2-fold increase in phosphorylated ninein in endothelial cells (supplemental Figure IIB and IIC).

To further investigate whether ninein is expressed in endothelial cells in vivo, we performed immunofluorescence staining of frozen sections from human kidney, kidney tumor, and inflammatory tumor stroma. Vessels were visualized by staining with FITC-conjugated UEA-1. We found a high cytoplasmic expression of ninein in endothelial cells in a subset of vessels in normal kidney (Figure 3A, arrowheads)

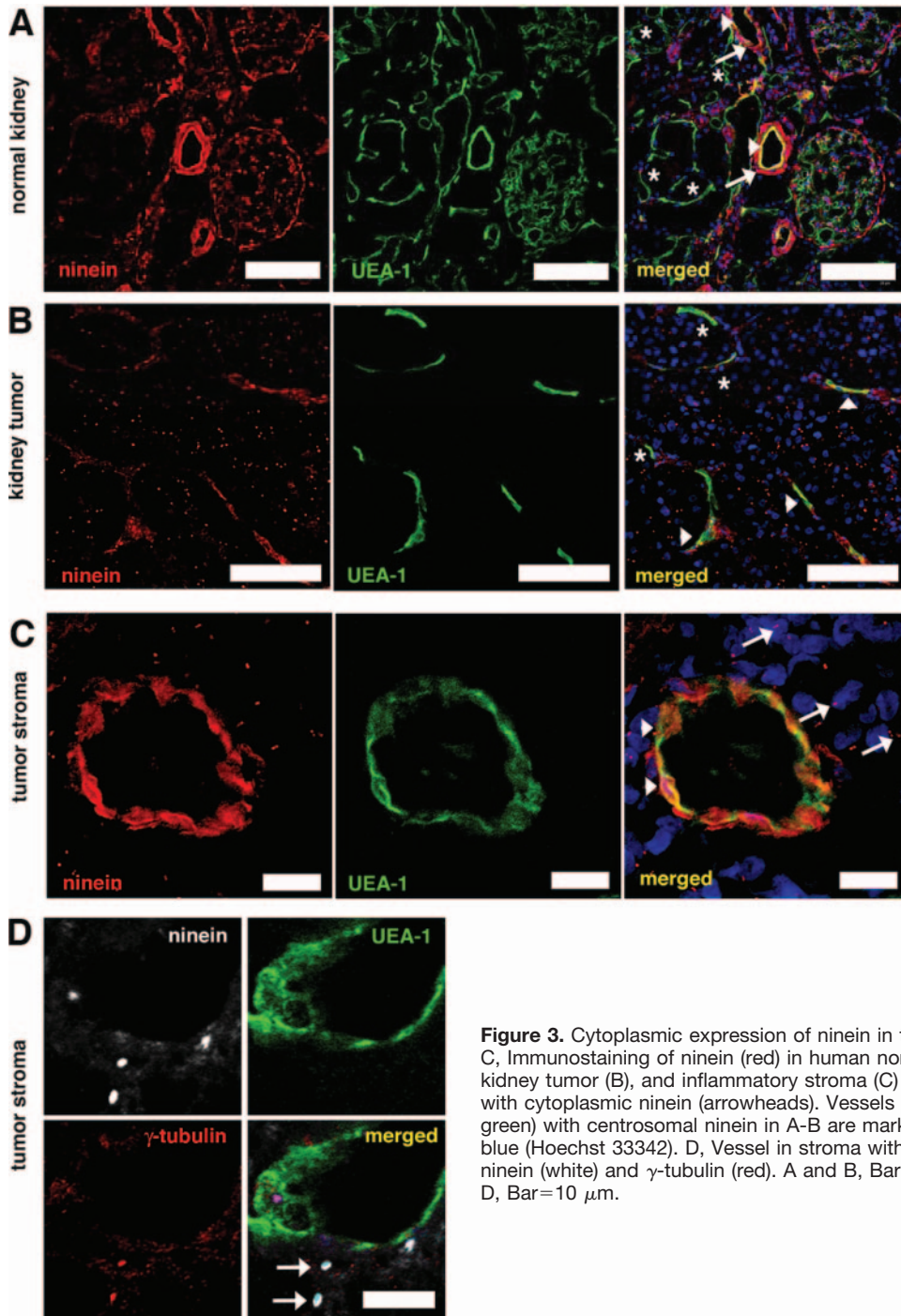


**Figure 3.** Cytoplasmic expression of ninein in tissues. A through C, Immunostaining of ninein (red) in human normal kidney (A), kidney tumor (B), and inflammatory stroma (C) shows vessels with cytoplasmic ninein (arrowheads). Vessels (UEA-1-positive, green) with centrosomal ninein in A-B are marked by (\*). Nuclei in blue (Hoechst 33342). D, Vessel in stroma with colocalization of ninein (white) and  $\gamma$ -tubulin (red). A and B, Bar=100  $\mu$ m. C and D, Bar=10  $\mu$ m.

and in pericytes/smooth muscle cells surrounding small arteries (Figure 3A, arrows). Similarly, kidney tumor vessels frequently expressed high levels of ninein in the cytoplasm (Figure 3B, arrowheads), whereas the surrounding tumor cells showed centrosomal localization of ninein. In the tumor stroma, endothelial cells in many vessels expressed high levels of ninein in the cytoplasm (Figure 3C, arrowheads). Notably, ninein was localized in the centrosome in the majority of normal vessels, whereas a varying proportion of tumor vessels and stromal vessels showed centrosomal localization of ninein (see asterisk in Figure 3A, 3B, and 3D). Nonendothelial cells in tumor and tumor stroma typically

displayed a centrosomal localization of ninein (Figure 3C, arrows). The centrosomal localization of ninein was verified through costaining with  $\gamma$ -tubulin (Figure 3D).

The cytoplasmic localization of ninein in many tumor vessels prompted further analyses on whether ninein was expressed in the cytoplasm of endothelial cells during vascular development. VEGF-induced vascularization of embryoid bodies, aggregates of differentiating mouse embryonic stem cells, largely mimics vasculogenesis and angiogenesis in the mouse embryo.<sup>18</sup> Immunostaining of embryoid bodies revealed a high cytoplasmic expression of ninein in CD31-positive blood vessels (Figure 4A). To further explore ninein-

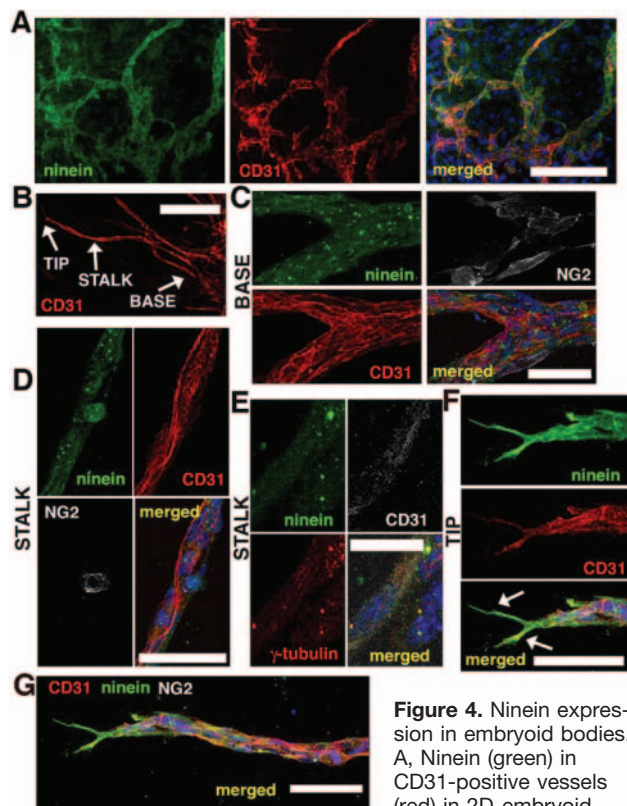


**Figure 4.** Ninein expression in embryoid bodies. A, Ninein (green) in CD31-positive vessels (red) in 2D-embryoid

body. Bar=100  $\mu$ m. B through E, Ninein in VEGF-induced sprouting in 3D-collagen. B, Overview showing the base, stalk, and tip of the growing sprout. Bar=200  $\mu$ m. C, Centrosomal localization of ninein in the base. NG2-positive pericytes (white). Bar=50  $\mu$ m. D, Centrosomal and cytoplasmic localization of ninein in the stalk. Bar=50  $\mu$ m. E, Colocalization of ninein (green) with  $\gamma$ -tubulin (red) in the stalk. Bar=25  $\mu$ m. F, G, Cytoplasmic localization of ninein in tip cell. Bar=50  $\mu$ m.

expression during sprouting angiogenesis, we seeded embryoid bodies in a 3D collagen matrix and treated with VEGF for 12 days. In this model, endothelial cells migrate into the surrounding gel and form lumen-containing vessel structures that are guided by a nonproliferating tip-cell (overview of CD31-positive sprouts shown in Figure 4B). A clear centrosomal localization of ninein was seen in the base of the endothelial sprout, although ninein was also distributed in the cytoplasm (Figure 4C). In the stalk, ninein was found in the centrosomes and cytoplasm of endothelial cells, as well as in NG2-positive pericytes (Figure 4D). This is in accordance with the cytoplasmic localization of ninein we detected in smooth muscle cells surrounding arteries eg, in the kidney (Figure 3A). Centrosomal localization of ninein was confirmed by costaining with  $\gamma$ -tubulin in the stalk (Figure 4E). Interestingly, the most prominent cytoplasmic localization of ninein was found in the angiogenic tip-cell (Figure 4F, overview of sprout shown in 4G). Filopodia extending from the tip-cell showed exceptionally strong ninein expression (Figure 4F, arrows), compatible with a role for ninein in endothelial cell path-finding. Interestingly, we found both actin and  $\alpha$ -tubulin expression in filopodia of tip-cells, suggesting that microtubules are involved in this process (supplemental Figure III).

To determine whether ninein expression is required for endothelial differentiation to create vessel structures, ninein expression was silenced by siRNA targeting in TIME cells before VEGF-induced tubular morphogenesis. Ninein expression was efficiently attenuated by 2 different siRNAs, Nin1 and Nin2, as determined by RT-PCR (Figure 5A) and Western blot analysis (Figure 5B). Introduction of ninein siRNA led to decreased proliferation of endothelial cells, consistent with an important role of ninein in centrosomal function during mitosis (Figure 5C). Importantly, depletion of ninein in endothelial cells was associated with marked decrease in formation of tubular structures in response to VEGF (Figure 5D, quantified in 5E). Ninein siRNA-transfected cells failed to arrange in long tubular structures, and instead, often formed nonorganized aggregates (Figure 5D). Similarly, decreased formation of vessel-like structures after ninein siRNA-transfection was observed for FGF-2-treated BCE cells (data not shown).

## Discussion

Formation of the vascular tube requires dramatic changes in endothelial cell morphology, orchestrated by proteins that regulate the endothelial cytoskeleton. We found that the centrosomal protein ninein is expressed in the cytoplasm of endothelial cells during tubular morphogenesis in vitro and in the developing vasculature of embryoid bodies. Interestingly, depletion of ninein led to disruption of tubular morphogenesis. This was not attributable to inhibition of proliferation, as endothelial cells undergoing tubular morphogenesis are growth arrested.<sup>19</sup> Instead, ninein is likely to be involved in redistribution of the microtubule cytoskeleton important for migration and 3D organization of endothelial cells. In accordance, depletion of ninein is accompanied by disruption of the microtubule array, suggesting that ninein is required for maintaining cell shape.<sup>20</sup> Moreover, ninein overexpression interferes with recapture and release of microtubule minus-ends at the centrosome, with consequent inhibition of cell migration.<sup>15</sup>

Immunostaining of human renal cancer and healthy control tissue demonstrated abundant expression of ninein in the cytoplasm of endothelial cells in a subset of vessels, whereas other endothelial cells showed a clear centrosomal location of ninein. Interestingly, although ninein was found in the centrosome in endothelial cells in the base of vascular sprouts in 3D embryoid body cultures, it was predominantly located in the cytoplasm of sprouting tip cells. Ninein has been shown to target  $\gamma$ -tubulin to the centrosome, and overexpression of ninein leads to redistribution of  $\gamma$ -tubulin to noncentrosomal sites.<sup>21</sup> Accordingly, we often found diffuse cytoplasmic expression of  $\gamma$ -tubulin in endothelial cells with predominantly cytoplasmic ninein. We propose that cytoplasmic ninein is released from the centrosome during active angiogenesis, allowing minus-end anchoring of microtubules at noncentrosomal sites in endothelial cells (supplemental Figure IV). Redistribution of microtubule nucleation proteins, including ninein, has previously been associated with differentiation of lens epithelium and muscle cells,<sup>22,23</sup> and ninein resides in the cytoplasm in polarized cells such as developing neurons and epithelial cells.<sup>6,17,24</sup> Our data suggest that

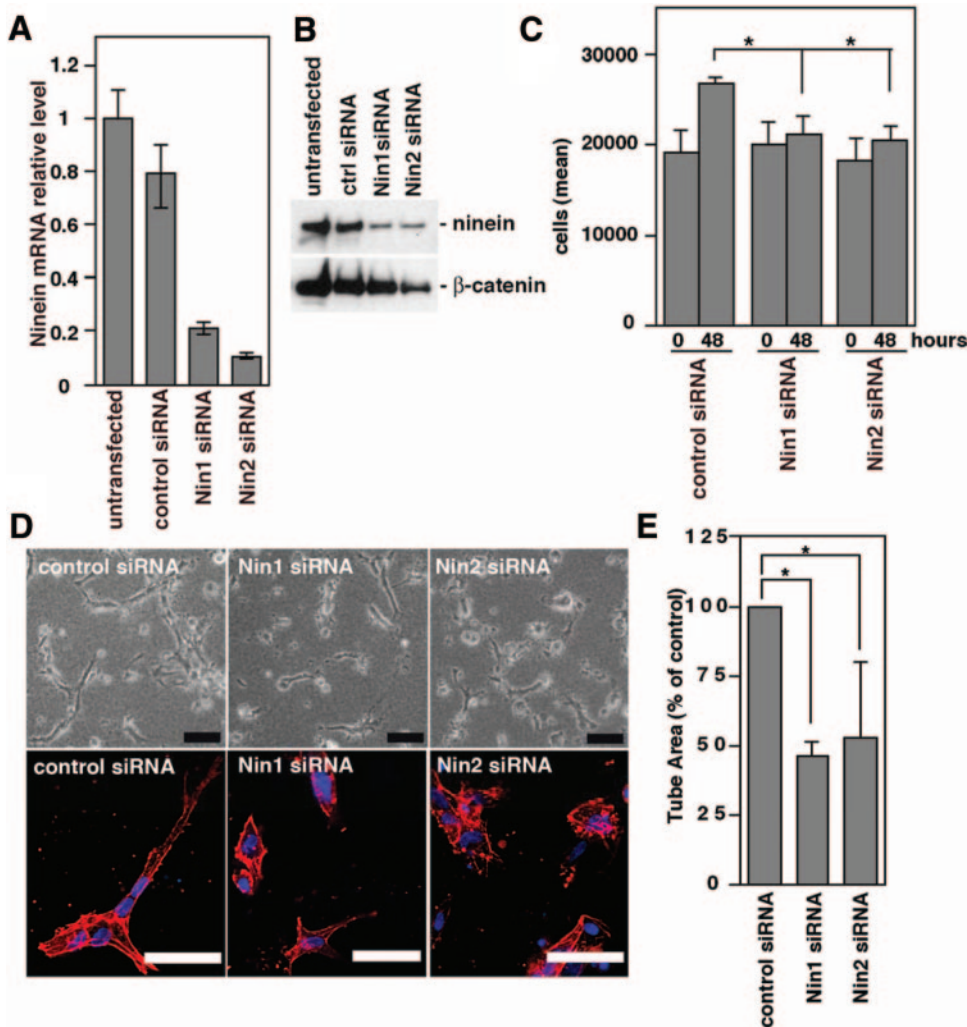


**Figure 5.** Ninein silencing inhibits VEGF-induced tubular morphogenesis. A and B, Ninein mRNA (A) and protein (B) in TIME cells treated with Nin1, Nin2, or control siRNAs. C, Cell numbers of siRNA-treated cells at seeding and after 48 hours. Mean  $\pm$  SD of triplicates. D, Tubular structures formed by control and ninein-siRNA-treated TIME cells (upper). Confocal images of phalloidin-Texas Red tubular structures (lower). Bar = 50  $\mu$ m. E, Quantification of tubular area (mean  $\pm$  SD, n = 4, \* $P$  < 0.05).

cytoplasmic ninein is instrumental in microtubule reorganization required for adaptation of endothelial cell morphology during angiogenesis. The extent of colocalization of ninein with  $\gamma$ -tubulin or microtubules was not always prominent, however, and we cannot formally exclude other functions for ninein in endothelial cells.

Microtubule-targeted drugs (MTD)s are widely used in anticancer treatment and have antimetabolic and antiangiogenic properties.<sup>25</sup> It has been shown that MTDs used as vascular disrupting agents specifically target tumor vasculature, suggesting a specific architecture of these vessels. Our results showing a cytoplasmic localization of ninein in many tumor vessels, may indeed reflect changes in patterning and/or stability of the microtubule network. Microtubule dynamics are modified by many different microtubule-interacting proteins, which are regulated by kinases and phosphatases downstream eg, growth factor signaling. Ninein interacts with GSK3 $\beta$ ,<sup>26</sup> and it has been shown that the coiled-coiled II domain can be phosphorylated by AuroraA and PKA.<sup>27</sup> In addition, ninein can be modified by SUMOylation, resulting in translocation from the centrosome to the nucleus.<sup>28</sup> We found that cytoplasmic ninein is tyrosine phosphorylated during tubular morphogenesis of endothelial cells. Of note, tyrosine phosphorylated ninein could not be detected in 293T

or U2OS cells, where it has a clear centrosomal localization. There are 20 tyrosine residues in human ninein. According to the NetPhos phosphorylation site prediction bioinformatic tool (<http://www.cbs.dtu.dk/services/NetPhos/>),<sup>29</sup> 10 of these are putative tyrosine phosphorylation sites. Future goals include to identify which tyrosine phosphorylation site(s) in ninein that are regulated during angiogenesis and to further investigate the function of ninein tyrosine phosphorylation in endothelial cells.

### Sources of Funding

This study was supported by the Association for International Cancer Research (AICR Grant 04-069), the Astrid Karlsson foundation, the Gustaf Adolf Johansson foundation, Svenska Sällskapet för Medicinsk Forskning, the Magnus Bergvall foundation, Nihon University Multidisciplinary Research Grant for 2008 (08-020), Swedish Research Council (project no. K2005-32X-12552-08A), and the Swedish Cancer Society (project 4828-B03-01PAA and 3820-B05-10XBC). The Fresh Tissue Biobank at Uppsala University Hospital was supported by the National Biobank Platform funded by Wallenberg Consortium North and Swegene.

### Disclosures

None.

## References

- Olsson AK, Dimberg A, Kreuger J, Claesson-Welsh L. VEGF receptor signalling - in control of vascular function. *Nat Rev Mol Cell Biol*. 2006; 7:359–371.
- Auguste P, Javerzat S, Bikfalvi A. Regulation of vascular development by fibroblast growth factors. *Cell Tissue Res*. 2003;314:157–166.
- Ribatti D, Vacca A, Nico B, Roncali L, Dammacco F. Postnatal vasculogenesis. *Mech Dev*. 2001;100:157–163.
- Papetti M, Herman IM. Mechanisms of normal and tumor-derived angiogenesis. *Am J Physiol Cell Physiol*. 2002;282:C947–C970.
- Bertolini F, Shaked Y, Mancuso P, Kerbel RS. The multifaceted circulating endothelial cell in cancer: towards marker and target identification. *Nat Rev Cancer*. 2006;6:835–845.
- Bouckson-Castaing V, Moudjou M, Ferguson DJ, Mucklow S, Belkaid Y, Milon G, Crocker PR. Molecular characterisation of ninein, a new coiled-coil protein of the centrosome. *J Cell Sci*. 1996;109(Pt 1): 179–190.
- Delgehr N, Sillibourne J, Bornens M. Microtubule nucleation and anchoring at the centrosome are independent processes linked by ninein function. *J Cell Sci*. 2005;118:1565–1575.
- Mogensen MM, Malik A, Piel M, Bouckson-Castaing V, Bornens M. Microtubule minus-end anchorage at centrosomal and non-centrosomal sites: the role of ninein. *J Cell Sci*. 2000;113:3013–3023.
- Dimberg A, Rylova S, Dieterich LC, Olsson AK, Schiller P, Wikner C, Bohman S, Botling J, Lukinius A, Wawrousek EF, Claesson-Welsh L. {alpha}B-crystallin promotes tumor angiogenesis by increasing vascular survival during tube morphogenesis. *Blood*. 2008;111:2015–2023.
- Venetsanakis E, Mirza A, Fanton C, Romanov SR, Tlsty T, McMahon M. Induction of tubulogenesis in telomerase-immortalized human microvascular endothelial cells by glioblastoma cells. *Exp Cell Res*. 2002;273: 21–33.
- Bohman S, Matsumoto T, Suh K, Dimberg A, Jakobsson L, Yuspa S, Claesson-Welsh L. Proteomic analysis of vascular endothelial growth factor-induced endothelial cell differentiation reveals a role for chloride intracellular channel 4 (CLIC4) in tubular morphogenesis. *J Biol Chem*. 2005;280:42397–42404.
- Nagy A, Rossant J, Nagy R, Abramow-Newerly W, Roder JC. Derivation of completely cell culture-derived mice from early-passage embryonic stem cells. *Proc Natl Acad Sci U S A*. 1993;90:8424–8428.
- Magnusson P, Rolny C, Jakobsson L, Wikner C, Wu Y, Hicklin DJ, Claesson-Welsh L. Deregulation of Flk-1/vascular endothelial growth factor receptor-2 in fibroblast growth factor receptor-1-deficient vascular stem cell development. *J Cell Sci*. 2004;117:1513–1523.
- Mack GJ, Rees J, Sandblom O, Balczon R, Fritzlner MJ, Rattner JB. Autoantibodies to a group of centrosomal proteins in human autoimmune sera reactive with the centrosome. *Arthritis Rheum*. 1998;41:551–558.
- Abal M, Piel M, Bouckson-Castaing V, Mogensen M, Sibarita JB, Bornens M. Microtubule release from the centrosome in migrating cells. *J Cell Biol*. 2002;159:731–737.
- Mogensen MM. Microtubule release and capture in epithelial cells. *Biol Cell*. 1999;91:331–341.
- Moss DK, Bellett G, Carter JM, Liovic M, Keynton J, Prescott AR, Lane EB, Mogensen MM. Ninein is released from the centrosome and moves bi-directionally along microtubules. *J Cell Sci*. 2007;120:3064–3074.
- Jakobsson L, Kreuger J, Claesson-Welsh L. Building blood vessels—stem cell models in vascular biology. *J Cell Biol*. 2007;177:751–755.
- Matsumoto T, Turesson I, Book M, Gerwins P, Claesson-Welsh L. p38 MAP kinase negatively regulates endothelial cell survival, proliferation, and differentiation in FGF-2-stimulated angiogenesis. *J Cell Biol*. 2002; 156:149–160.
- Dammermann A, Merdes A. Assembly of centrosomal proteins and microtubule organization depends on PCM-1. *J Cell Biol*. 2002;159: 255–266.
- Stillwell EE, Zhou J, Joshi HC. Human ninein is a centrosomal autoantigen recognized by CREST patient sera and plays a regulatory role in microtubule nucleation. *Cell Cycle*. 2004;3:923–930.
- Dahm R, Procter JE, Ireland ME, Lo WK, Mogensen MM, Quinlan RA, Prescott AR. Reorganization of centrosomal marker proteins coincides with epithelial cell differentiation in the vertebrate lens. *Exp Eye Res*. 2007;85:696–713.
- Bugnard E, Zaal KJ, Ralston E. Reorganization of microtubule nucleation during muscle differentiation. *Cell Motil Cytoskeleton*. 2005;60:1–13.
- Baird DH, Myers KA, Mogensen M, Moss D, Baas PW. Distribution of the microtubule-related protein ninein in developing neurons. *Neuropharmacology*. 2004;47:677–683.
- Jordan MA, Wilson L. Microtubules as a target for anticancer drugs. *Nat Rev Cancer*. 2004;4:253–265.
- Hong YR, Chen CH, Chang JH, Wang S, Sy WD, Chou CK, Howng SL. Cloning and characterization of a novel human ninein protein that interacts with the glycogen synthase kinase 3beta. *Biochim Biophys Acta*. 2000;1492:513–516.
- Chen CH, Howng SL, Cheng TS, Chou MH, Huang CY, Hong YR. Molecular characterization of human ninein protein: two distinct subdomains required for centrosomal targeting and regulating signals in cell cycle. *Biochem Biophys Res Commun*. 2003;308:975–983.
- Cheng TS, Chang LK, Howng SL, Lu PJ, Lee CI, Hong YR. SUMO-1 modification of centrosomal protein hNinein promotes hNinein nuclear localization. *Life Sci*. 2006;78:1114–1120.
- Blom N, Gammeltoft S, Brunak S. Sequence and structure-based prediction of eukaryotic protein phosphorylation sites. *J Mol Biol*. 1999;294: 1351–1362.